Computational Study of Radical Cations of Saturated Compounds with σ-Type and π-Type N−N Bonds

Jurriaan M. Zwier, Jochem Wichers Hoeth, and Albert M. Brouwer*,†

Institute of Molecular Chemistry, University of Amsterdam, Nieuwe Achtergracht 129, 1018 WS Amsterdam, The Netherlands

fred@org.chem.uva.nl

Received August 11, 2000

Geometrical and electronic properties have been calculated and are compared with experimental data for three saturated diaza compounds and their radical cations and dications. The molecular geometries in the different oxidation states are consistently reproduced very well using the B3PW91 and B3LYP three-parameter density functional methods, with a modest 6-31G* basis set. The performance of the pure density functionals BLYP and BPW91 is less satisfactory. The Hartree−Fock method yields excellent results in some cases but poor results in others. Ionization potentials and electron−nuclear hyperfine interactions are reproduced moderately well with B3LYP and B3PW91. Electronic excitation energies calculated with time-dependent density functional theory agree very well with experiment in most cases. For 2,7-diazatetracyclo[6.2.2.2^{3,6}.0^{2,7}]tetradecane **2** and its radical cation and dication, the reorganization parameters for self-electron exchange were calculated and compared with experimental and earlier computed data. The calculations allow a good estimate of the different contributions to the energy barrier, i.e., the internal and solvent reorganization energies and the work term in the case of **2**+/**2**++.

Introduction

In recent years, density functional theory (DFT) has become a very popular approach to molecular quantum chemical calculations.[1] Since the introduction of nonlocal gradient corrected functionals at the end of the 1980s,[2,3] molecular structures and properties can be calculated with an accuracy that is comparable to that of more costly traditional ab initio methods. Especially hybrid Hartree−Fock DFT methods (such as B3LYP)[4] show a very good performance at a modest computational cost.[5] In contrast to Hartree−Fock theory (HF), DFT methods perform well for organic radicals as well.[6−9] Some serious problems with the use of B3LYP on open-shell systems have, however, been noted. Bally and Sastry[10] showed that DFT methods applied to small radical ions tend to delocalize spin and charge too much, which leads to incorrect dissociation behavior in H_2^+ and He_2^+. A similar problem arises with the ammonia dimer radical cation: DFT calculations systematically overestimate the dissociation energy, and the length of the three electron bond is predicted to be too long.[11,12] Sodupe et al.[13] made similar observations for the water dimer radical cation and pointed out that the cause of the problem is inherent in DFT.

We have recently studied a number of radical cations, using spectroscopic methods and ab initio and DFT calculations, in which delocalization of charge and spin occurs through σ bonds, e.g. 1,4-dimethylpiperazine and 1,4-diaza[2.2.2]bicyclooctane radical cations.[14−20] The results of the DFT calculations in those cases were in excellent agreement with the spectroscopic data and allowed a detailed interpretation of the latter. In other cases, in which through-bond delocalization of charge and spin is less favored,[19,21] or may compete with through space interactions leading to a three-electron bond (e.g., in boat structures for piperazine radical cations),[16] the tendency of DFT toward delocalization may lead to incorrect predictions. It therefore remains necessary to test the validity of the results of DFT calculations for different open-shell systems for which reliable experimental data are available.

† Fax +31205255670. Phone +31205255491.

(1) Koch, W.; Holthausen, M. C. *A chemist's guide to density functional theory: an introduction and practical guide to DFT calculations*; Wiley-VCH: Weinheim, 2000.
(2) See, for example: St-Amant, A. Density functional methods in biomolecular chemistry. In *Reviews in Computational Chemistry*; Lipkowitz, K. B., Boyd, D. B., Eds.; Wiley: New York; Vol. 7, p 217.
(3) Becke, A. D. *J. Comput. Chem.* **1999**, *20*, 63.
(4) Becke, A. D. *J. Chem. Phys.* **1993**, *98*, 5648.
(5) Curtiss, L. A.; Raghavachari, K.; Redfern, R. C.; Pople, J. A. *Chem. Phys. Lett.* **1997**, *270*, 419.
(6) Qin, Y.; Wheeler, R. A. *J. Chem. Phys.* **1995**, *102*, 1689.
(7) Brouwer, A. M. *J. Phys. Chem. A* **1997**, *101*, 3626.
(8) Vereecken, L.; Peeters, J. *J. Phys. Chem.* **1999**, *103*, 1768.
(9) Baldridge, K. K.; Leahy, J.; Siegel, J. S. *Tetrahedron Lett.* **1999**, *40*, 3503.
(10) Bally, T.; Sastry, G. N. *J. Phys. Chem. A* **1997**, *101*, 7923.
(11) Havenith, R. Utrecht University, personal communication.
(12) Braïda, B.; Hiberty, P. C.; Savin, A. *J. Phys. Chem. A* **1998**, *102*, 7872.
(13) Sodupe, M.; Bertran, J.; Rodrigues-Santiago, L.; Baerends, E. J. *J. Phys. Chem. A* **1999**, *103*, 166.
(14) Zwier, J. M.; Wiering, P. G.; Brouwer, A. M.; Bebelaar, D.; Buma, W. J. *J. Am. Chem. Soc.* **1997**, *119*, 11523.
(15) Brouwer, A. M.; Wiering, P. G.; Zwier, J. M.; Langkilde, F. W.; Wilbrandt, R. *Acta Chem. Scand.* **1997**, *51*, 217.
(16) Brouwer, A. M.; Zwier, J. M.; Svendsen, C.; Mortensen, O. S.; Langkilde, F. W.; Wilbrandt, R. *J. Am. Chem. Soc.* **1998**, *120*, 3748.
(17) Brouwer, A. M.; Svendsen, C.; Mortensen, O. S.; Wilbrandt, R. *J. Raman Spectrosc.* **1998**, *29*, 439.
(18) Balakrishnan, G.; Keszthelyi, T.; Wilbrandt, R.; Zwier, J. M.; Brouwer, A. M.; Buma, W. J. *J. Phys. Chem. A* **2000**, *104*, 1834.
(19) Zwier, J. M.; Brouwer, A. M.; Balakrishnan, G.; Keszthelyi, T.; Offersgaard, J. F.; Wilbrandt, R. Manuscript in preparation.
(20) Zwier, J. M.; Brouwer, A. M.; Keszthelyi, T.; Offersgaard, J. F.; Wilbrandt, R.; Barbosa, F.; Buser, U.; Gescheidt, G.; Nelsen, S. F.; Little, C. D. Manuscript in preparation.
(21) Zwier, J. M. Ph.D. Thesis, University of Amsterdam, 2000.

10.1021/jo005605s CCC: $20.00
Published on Web 12/29/2000

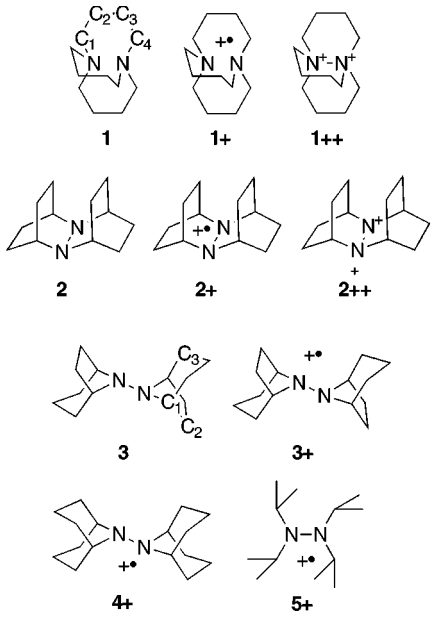

Figure 1. Structures of the molecules studied.

In the present paper we focus on cases in which direct through-space interactions between two nitrogen atoms occur. We will compare the results of a variety of DFT and hybrid HF/DFT methods with crystal structures and other experimental data of neutral and one-electron or two-electron oxidized diamines and hydrazines **1**, **2**, and **3** (Figure 1). Although several alkylamines are known to have stable cations, we have chosen to investigate these three compounds, which have been studied predominantly in the groups of Alder[22] and Nelsen,[23] because of the availability of a variety of experimental data and because they contain (semi) rigid ring structures, like the compounds studied in our own work. Furthermore, each of them represents a different class of "diamine".

The most interesting geometrical property of these systems is the N−N distance, as it is strongly influenced by the electronic coupling between the nitrogen atoms and steric constraints imposed by the polycyclic framework. In addition to the geometry, properties such as vertical ionization potentials, vertical excitation energies, and internal reorganization energies for self-exchange electron transfer are calculated and compared with experimental and computed data previously reported.

Crystal structural data are available for 1,6-diazabicyclo[4.4.4]tetradecane **1**,[24] its radical cation **1**+,[25] and its dication **1**++.[25] This diamine has been very well studied because of its special geometry. The nitrogen lone pairs point inward, toward each other, and form a two-center three-electron bond in the radical cation and a covalent σ-bond in the dication, respectively. Two types of hydrazines were studied. 2,7-Diazatetracyclo[6.2.2.2^{3,6}.0^{2,7}]-tetradecane **2**[26,27] and its radical cation **2**+ and dication **2**++ represent three oxidation states of a tetracyclic restrained hydrazine in which the nitrogen lone pairs are forced into an unfavorable position (π-type overlap). The second hydrazine series consists of 8,8′-bis-8-azabicyclo-[3.2.1]octane **3** and its radical cation **3**+.[28] In **3**, the lone pairs are also forced into an electronically unfavorable position due to the bulky bicyclic units. With those three compounds in hand, we can make a comparison between various ab initio methods. We chose HF, BLYP, BPW91, B3PW91, and B3LYP with the 6-31G* basis set as the set of standard methods available in several ab initio programs.[29,30] The possibility of basis set dependence of the results was tested for B3LYP calculations of the **1** series using the 6-311G** basis set and the correlation consistent cc-pVDZ basis set.[31]

Results and Discussion

1,6-Diazabicyclo[4.4.4]tetradecane (1). One of the characteristic geometrical features of diamine **1** is the inward positioning of nitrogen lone pairs, enforced by the stability of the chair conformation of the (pseudo) six-membered rings, as schematically indicated in Figure 1. For **1**+ and **1**++ this geometry is stabilized by the overlapping nitrogen lone pairs forming a two-center three-electron bond in the radical cation and a covalent bond in the dication, respectively. This is clearly shown in the orbital picture (Figure 2) for the three oxidation states.

Compound **1** is very sensitive to air as a solid[32] and is only stable for a few hours, whereas **1**+(•BF_4^-) is indefinitely stable as a solid as well as in nonbasic solutions. The dication **1**++(•2BF_4^-) is stable as a solid and in acidic aqueous solution.[32] All structures have (near) D_3 symmetry in their solid state.[24,25] The computed structures all have D_3 symmetry. The results for **1**, **1**+, and **1**++ at the B3PW91/6-31G* level of theory are listed in Table 1. Complete data for the other methods are reported in the Supporting Information (Tables S1−S3).

Comparing the results of the different methods for **1** we note that the traditional HF calculation performs very well. It estimates the bond lengths best, together with the B3PW91 method. The N−N distance is calculated to be 0.04−0.08 Å greater than the experimental value. The

(22) Alder, R. W. *Tetrahedron* **1990**, *46*, 683.
(23) Nelsen, S. F.; Chen, L.-J.; Powell, D. R.; Neugebauer, F. A. *J. Am. Chem. Soc.* **1995**, *117*, 11434.
(24) Alder, R. W.; Orpen, A. G.; Sessions, R. B. *J. Chem. Soc., Chem. Commun.* **1983**, 999.
(25) Alder, R. W.; Orpen, A. G.; White, J. M. *J. Chem. Soc., Chem. Commun.* **1985**, 949.
(26) Nelsen, S. F.; Blackstock, S. C.; Frigo, T. B. *J. Am. Chem. Soc.* **1984**, *106*, 3366.
(27) Nelsen, S. F.; Frigo, T. B.; Kim, Y.; Thompson-Colón, J. A. *J. Am. Chem. Soc.* **1986**, *108*, 7926.
(28) Nelsen, S. F.; Cunkle, G. T.; Evans, D. H.; Haller, K. J.; Kaftory, M.; Kirste, B.; Kurreck, H.; Clark, T. *J. Am. Chem. Soc.* **1985**, *107*, 3829.
(29) Gaussian 94, Revisions D.1 and D.4. Frisch, M. J.; Trucks, G. W.; Schlegel, H. B.; Gill, P. M. W.; Johnson, B. G.; Robb, M. A.; Cheeseman, J. R.; Keith, T.; Petersson, G. A.; Montgomery, J. A.; Raghavachari, K.; Al-Laham, M. A.; Zakrzewski, V. G.; Ortiz, J. V.; Foresman, J. B.; Cioslowski, J.; Stefanov, B. B.; Nanayakkara, A.; Challacombe, M.; Peng, C. Y.; Ayala, P. Y.; Chen, W.; Wong, M. W.; Andres, J. L.; Reprogle, E. S.; Gomperts, R.; Martin, R. L.; Fox, D. J.; Binkley, J. S.; Defrees, D. J.; Baker, J.; Stewart, J. J. P.; Head-Gordon, M.; Gonzales, C.; Pople, J. A. Gaussian, Inc.: Pittsburgh, PA, 1995.
(30) Gaussian 98, Revisions A.5 and A.7. Frisch, M. J.; Trucks, G. W.; Schlegel, H. B.; Scuseria, G. E.; Robb, M. A.; Cheeseman, J. R.; Zakrzewski, V. G.; Montgomery, J. A., Jr.; Stratmann, R. E.; Burant, J. C.; Dapprich, S.; J. M. Millam; Daniels, A. D.; Kudin, K. N.; Strain, M. C.; Farkas, O.; Tomasi, J.; Barone, V.; Cossi, M.; Cammi, R.; Mennucci, B.; Pomelli, C.; Adamo, C.; Clifford, S.; Ochterski, J.; Petersson, G. A.; Ayala, P. Y.; Q. Cui; Morokuma, K.; Malick, D. K.; Rabuck, A. D.; Raghavachari, K.; Foresman, J. B.; Cioslowski, J.; Ortiz, J. V.; Stefanov, B. B.; Liu, G.; Liashenko, A.; Piskorz, P.; Komaromi, I.; Gomperts, R.; Martin, R. L.; Fox, D. J.; Keith, T.; Al-Laham, M. A.; Peng, C. Y.; Nanayakkara, A.; Gonzalez, C.; Challacombe, M.; Gill, P. M. W.; Johnson, B.; Chen, W.; Wong, M. W.; Andres, J. L.; Gonzalez, C.; Head-Gordon, M.; Replogle, E. S.; Pople, J. A. Gaussian, Inc.: Pittsburgh, PA, 1998.
(31) Dunning, T. H., Jr. *J. Chem. Phys.* **1989**, *90*, 1007.
(32) Alder, R. W.; Sessions, R. B. *J. Am. Chem. Soc.* **1979**, *101*, 3651.

Table 1. Experimental and Calculated Features at the B3PW91/6-31G* Level[a] of 1,6-diazabicyclo[4.4.4]tetradecane 1, Its Radical Cation 1+ and Dication 1++

	neutral molecule **1**		radical cation **1**+		dication **1**++	
	exp[b]	B3PW91	exp[c]	B3PW91	exp[d]	B3PW91
r(N−N)	2.806(3)	2.844	2.295(10)	2.370	1.532(6)	1.537
r(N−C_1)	1.443(3)	1.446	1.466(11)	1.469	1.533(6)	1.539
r(C_1−C_2)	1.521(4)	1.535	1.509(12)	1.527	1.505(8)	1.518
r(C_2−C_3)	1.521(4)	1.538	1.509(12)	1.527	1.505(8)	1.524
∠(C_1-N−$C_{1'}$)	115.5(2)	115.8	114.0(6)	113.7	109.0(4)	108.6
∠(N−C_1−C_2)	114.1(2)	114.9	115.6(7)	115.3	114.2(4)	114.5
∠(C_1−C_2−C_3)	116.3(2)	116.6	115.0(8)	114.7	111.0(4)	110.8
ΣN	346.5	347.4	342.0	341.0	327.0	325.9
∠(C_1-N−N′−C_4)	18.2(2)	19.5	38.8(7)	34.5	52.2(4)	51.6
∠(N−N′−C_1−C_2)	−30.6(2)	−31.5	−44.8(8)	−42.0	−54.6(5)	−54.2
∠(N−C_1−C_2−C_3)	68.2(2)	67.9	63.3(10)	64.5	54.8(6)	54.5
∠(C_1-C_2−C_3−C_4)	−90.1(2)	−87.9	−66.9(10)	−71.1	−53.0(6)	−52.7
IP_v (eV)	6.75	6.16[e]				
ESR data						
a_N(2)			34.4	30.2		
a_H(6)			17.2	17.2		
exc. energy (eV)			2.6	2.38[f]		
exc. energy (eV)			2.6	2.78(0.16)[g]		

[a] Results obtained with HF, B3LYP (different basis sets), BLYP, and BPW91 can be found in the Supporting Information (Tables S1−S3). [b] Crystallographic data from Alder et al.[24] with estimated deviation in the least significant digit. For atom numbering see Figure 1. For the bonds C_1−C_2 and C_2−C_3 averaged values are reported. Bond distances in Å, angles in degrees. Symmetry D_3. Vertical ionization potential reported by Alder et al.[33] [c] Crystallographic data and ESR splitting constants (Gauss) from Alder et al.[25] of **1**+(•ClO_4^-). Excitation energies from refs 32 and 35. [d] Crystallographic data of **1**++(•2$CF_3SO_3^-$) from Alder et al.[25] [e] Difference between the energy of the radical cation and that of the neutral molecule at the optimized geometry of the latter. [f] ΔSCF method. [g] TDDFT, oscillator strength in parentheses.

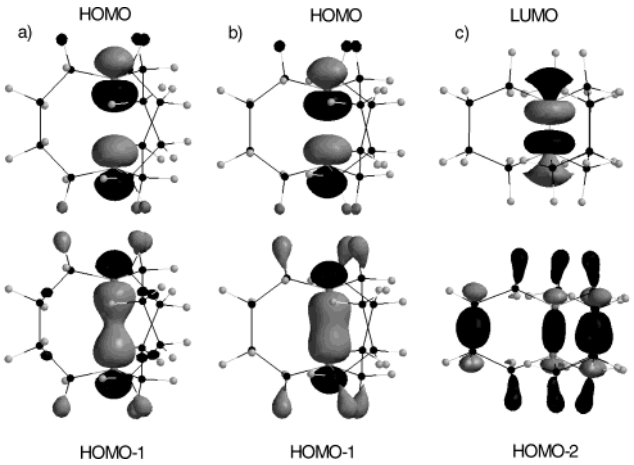

Figure 2. N−N bonding and antibonding molecular orbitals of 1,6-diazabicyclo[4.4.4]tetradecane **1** neutral (a), radical cation **1**+ (b), and dication **1**++ (c).

B3PW91 method may be expected to be the best hybrid DFT method because in the original work of Becke[4] the three-parameter combination of the Becke exchange functional, exact exchange, and correlation functionals was optimized with the PW91 correlation functional. Later, other authors replaced the PW91 with the LYP correlation functional, and the resulting B3LYP method has quickly become established as a standard, even though the parameters are not necessarily optimal. The hybrid HF/DFT methods perform better than their pure DFT counterparts, which is in line with general experience. Improving the basis set in the B3LYP calculation from 6-31G* to cc-pVDZ leads to more accurate results, but the effect is marginal and not worth the added computational effort. Bond angles and dihedral angles are predicted quite well by all seven methods.

For **1**+ the HF calculation gives a significantly better estimation of the N−N distance than the DFT methods. The HF value is just 0.02 Å smaller than the experimental result while the pure DFT methods overestimate the distance by 0.08−0.21 Å. These errors are similar to those found for the ammonia dimer radical cation.[12] The other bond lengths are also well predicted by HF theory, although B3PW91 performs equally well and appears to be the most accurate of the DFT-based methods. Also here, the hybrid DFT methods yield better values than their pure DFT analogues. The bond angles calculated with the DFT methods are somewhat closer to the experimental values than those from HF theory, especially for the C−N−C angle. As a result of this, DFT yields a better description of the pyramidalization of the nitrogen atoms, which can be measured via the sum of the bond angles of the N atom, denoted as ΣN.

The ESR hyperfine coupling constants of **1**+ have been measured by Alder et al.[32,36] The unusually large hyperfine coupling of the nitrogen atoms of 34.4 G is consistent with strong inward pyramidalization. There is also a large splitting found for the six equivalent equatorial α-hydrogens of 17.2 G. Hyperfine splitting constants can be predicted reasonably accurately using DFT methods, as was shown by Batra et al.[37] for various radicals, including hydrazine radical cations. The splitting constant a_N calculated with HF of 48.5 G is much larger than the experimentally observed value. On the other hand, the pure DFT methods underestimate the nitrogen splittings by about 25%. The B3LYP and the B3PW91 methods again perform best, reproducing the hydrogen splitting exactly and underestimating the nitrogen splitting slightly. Extending the basis set from 6-31G* to cc-pVDZ does not lead to more accurate results. Although the nitrogen splitting calculated with B3LYP/cc-pVDZ is

(33) Alder, R. W.; Arrowsmith, R. J.; Casson, A.; Sessions, R. B.; Heilbronner, E.; Kovac, B.; Huber, H.; Taagepera, M. *J. Am. Chem. Soc.* **1981**, *103*.

(34) Howard, S. T.; Platts, J. A.; Alder, R. W. *J. Org. Chem.* **1995**, *60*, 6085.

(35) Nelsen, S. F.; Alder, R. W.; Sessions, R. B.; Asmus, K.-D.; Hiller, K.-O.; Göbl, M. *J. Am. Chem. Soc.* **1980**, *102*, 1429.

(36) Kirste, B.; Alder, R. W.; Sessions, R. B.; Bock, M.; Kurreck, H.; Nelsen, S. F. *J. Am. Chem. Soc.* **1985**, *107*, 2635.

(37) Batra, R.; Giese, B.; Spichty, M.; Gescheidt, G.; Houk, K. N. *J. Phys. Chem.* **1996**, *100*, 18371.

Table 2. Experimental[a] and Calculated Properties (B3PW91/6-31G*)[b] of 2,7-Diazatetracyclo[6.2.2.2^{3,6}.0^{2,7}] Tetradecane (2) and Its Radical Cation and Dication

	neutral **2**[c]		radical cation **2**+[d]		dication **2**++[e]	
	exp	B3PW91	exp	B3PW91	exp	B3PW91
r(N−N)	1.492	1.479	1.325	1.343	1.270	1.274
r(C−N)	1.478	1.471	1.472	1.467	1.471	1.468
∠(C_1−N−N)	111.0	111.2	114.4	114.1	115.8	115.8
∠(C_4−N−N)	108.7	109.5				
∠($C_{4'}$−N−C_1)	118.6	120.0	126.0	129.2	128.5	128.5
∠(C_1−N−N−$C_{1'}$)	117.2	121.2	161.0	163.0		
∠(C_4−N−N−$C_{4'}$)	147.2	148.5				
∠(C_1−N−N−C_4)	15.0	13.6				
a_N(2)			15.2	12.9		

[a] Crystallographic data from Nelsen et al. for **2**, **2**+(•TsO$^-$), and **2**++(•2PF$_6^-$).[42] For atom numbering see Figure 3. Bond distances in Å, angles in degrees. Hyperfine interaction constant in Gauss, from ref 42. [b] For data obtained with HF, B3LYP, BLYP, and BPW91, see Supporting Information (Table S4). [c] C_2 symmetry. [d] C_{2v} symmetry. [e] D_{2h} symmetry.

closest to the experimentally determined value, the α-hydrogen coupling is reproduced only poorly.

All radical cations discussed in this paper have an electronic transition corresponding to a simple one-electron excitation, i.e., (HOMO-1)^2(HOMO)^1 → (HOMO-1)^1(HOMO)^2 (see Figure 2). This electronic transition for **1**+ is quite strong and shows up in the visible region. Alder and Sessions[32] reported an extremely broad band with λ_{max} = 480 nm (oscillator strength 0.1); in a later paper Nelsen et al. gave λ_{max} = 470 nm (ϵ = 4500 M^{-1} cm^{-1}).[35] The absorption maximum of the radical cation can be estimated by a simple "ΔSCF" approach: because HOMO-1 (a_1) and HOMO (a_2) belong to different irreducible representations, the excited state is the lowest state of its symmetry and can be described using the self-consistent field method. The energy difference with respect to the ground state of the radical cation can be taken as the excitation energy. This method works nicely for **1**+. The B3PW91 method predicts the excitation energy best. Its value of 2.38 eV is only 10% lower than the experimental value. A similar underestimation of the excitation energy was also observed for the radical cation of 1,4-dimethylpiperazine.[16] Improving the basis set for the B3LYP calculation has a negligible effect on the computed excitation energy. Pure DFT methods underestimate the excitation energy considerably, whereas the HF method overestimates it. Recently, time-dependent DFT methods[38−40] have become available for the calculation of excited-state properties. The experience with the performance of these methods is still limited. In the case of **1**+, we tested the B3LYP and B3PW91 functionals, with very satisfactory results, as shown in the last row of Table 1. The excitation energy computed using B3LYP/6-31G* is virtually identical to the experimental one; B3PW91 overestimates the excitation energy slightly.

HF overestimates the N−N bonding interaction in **1**++, predicting a bond length of 1.49 Å, significantly smaller than the experimental value of 1.53 Å. The pure DFT methods BLYP and BPW91, on the other hand, predict significantly larger values of 1.61 and 1.58 Å, respectively. The hybrid HF/DFT methods are very accurate indeed, with B3PW91 performing best again. The other bond lengths and angles are also best calculated using the B3PW91 method.

2,7-Diazatetracyclo[6.2.2.2^{3,6}.0^{2,7}]tetradecane (2). A. Geometrical Features. Only a few stable radical cations of alkylhydrazines are known, because decomposition by C$_\alpha$−H bond cleavage limits their stability.[41] By introducing steric strain on the hydrazine using bicyclic systems or sterically crowded groups, proper alignment

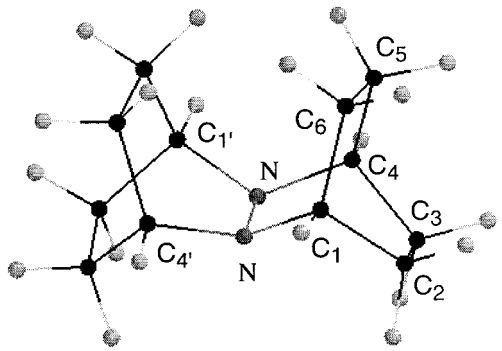

Figure 3. Structure of compound **2** with atom numbering (B3LYP/6-31G*).

of their N lone pairs with the C$_\alpha$−H bond is prevented. This stabilizes their radical cations. One of the peculiar properties of **2** is its ease of oxidation. It is one of the most easily oxidized hydrazines known with $E_{1/2}$(**2**,**2**+) of −0.53 vs SCE.[26] Crystal structural data of **2**, **2**+, and **2**++ are available.[42] Unfortunately, the structure of **2**+(TsO$^-$) could not be solved with high precision. Two unique but quite similar cation fragments were found in the unit cell. The average values over both species are given in Table 2, as the experimental values.

The frontier molecular orbitals of **2** are visualized in Figure 4. The HOMO-1 of the neutral shows π-bonding behavior due to the small angle between the nitrogen lone pairs. The HOMO, however, has π-antibonding character. In addition, there is steric strain due to nonbonding interactions in the bicyclic framework. As a result, the N−N bond in **2** is twisted to an angle of 15°, leading to a C_2 symmetric structure (see Figure 3). This twist angle is best reproduced by the B3PW91 method, which yields a value of 13.6° (Table 2). The other methods lead to smaller twist angles, the worst being the BLYP method. B3LYP performs best in predicting the N−N distance; the largest error is found for the HF calculation. Bond angles are predicted equally well for both hybrid DFT methods. The HF calculation leads to the largest deviations. Besides this twisted structure, a C_{2v} symmetric

(38) Casida, M. E.; Casida, K. C.; Salahub, D. R. *Int. J. Quantum Chem.* **1998**, *70*, 933.
(39) Stratmann, R. E.; Scuseria, G. E.; Frisch, M. J. *J. Chem. Phys.* **1998**, *109*, 8218.
(40) Handy, N. C.; Tozer, D. J. *J. Comput. Chem.* **1999**, *20*, 106.
(41) Nelsen, S. F.; Chen, L.-J.; Petillo, P. A.; Evans, D. H.; Neugebauer, F. A. *J. Am. Chem. Soc.* **1993**, *115*, 10611.
(42) Nelsen, S. F.; Blackstock, S. C.; Haller, K. J. *Tetrahedron* **1986**, *42*, 6101.

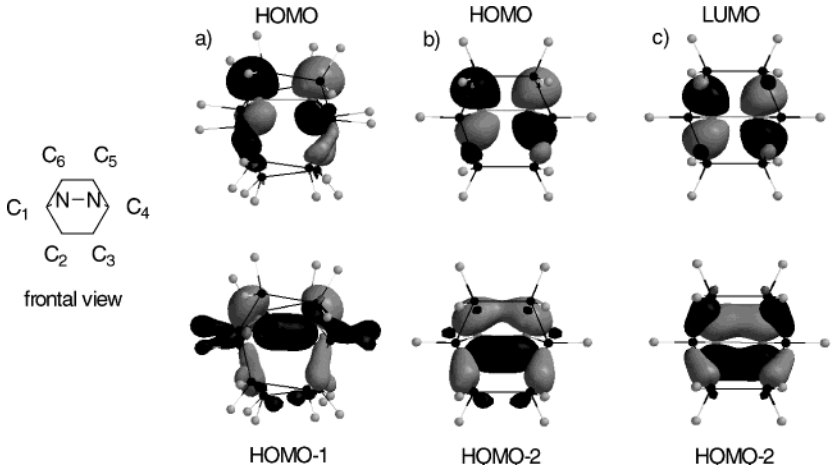

Figure 4. N−N bonding and antibonding molecular orbitals of 2,7-diazatetracyclo[6.2.2.2^{3,6}.0^{2,7}]tetradecane **2** (a), radical cation **2**+ (b), and dication **2**++ (c).

structure was also found. This structure corresponds to an energy minimum at the HF level but is a transition structure according to B3LYP. Its energy is computed to be higher than that of the C_2 structure by 0.9 and 0.6 kcal/mol using HF and B3LYP, respectively. Earlier semiempirical calculations on **2**[27,42−44] led to a structure of D_{2h} symmetry.

When **2** is oxidized to **2**+, an electron is removed from an antibonding π orbital leading to a net π-bonding interaction between the nitrogens (see Figure 4, part b), which causes a reduction of the twist angle. The lowest energy transition in the absorption spectrum of the cation (recorded in acetonitrile with three different counterions) is an electronic transition due to the promotion of an electron from the filled π-orbital to the singly occupied π^* orbital and appears at 264−266 nm (ϵ 1600−1800 M^{-1} cm^{-1}).[26] Time-dependent density functional calculations (B3LYP/6-31G*) predict an absorption maximum for this transition at 260 nm, with a modest oscillator strenght of 0.05. In addition, the calculation predicts two slightly weaker bands at 252 and 243 nm, but these are not resolved in the experimental spectrum, which shows a single band at 243−244 nm (ϵ 1500−1700 M^{-1} cm^{-1}).[27]

The crystallographic unit cell of **2**+ contains two molecules, which are similar and slightly distorted from C_{2v} symmetry. In our calculations of **2**+, only a C_{2v} symmetric syn-bonded structure was found even after optimizing from a twisted C_2 structure. Considering all geometrical features, the B3PW91 method performs best again although the N−N and C−N distances are predicted more accurately by the HF method. HF however fails to reproduce the C_1−N−N−$C_{1'}$ dihedral angle, making an error of 8°. It also miscalculates the nitrogen ESR splitting constant considerably (25 G). The experimental ESR nitrogen splitting constant of 15.2 G[27] (measured in acetonitrile solution) is calculated best with the B3LYP method (13.7 G). The predictions of the other DFT methods agree reasonably well with experiment. It is well-known that stronger pyramidalization of the nitrogens in amine radical cations is correlated with larger interaction between the electronic and ^{14}N nuclear spins.[37] In this case, the predicted pyramidalization is somewhat larger than that found experimentally, but the splitting constant is smaller than the experimental value.

After removal of a second electron, the nitrogens are completely flattened, and a full π-bond is formed, leading to a D_{2h} symmetric structure for **2**++. The N−N distance is shortened by another 0.06 Å compared with **2**+. The HF prediction of the structure is now far off, as was found earlier for **1**++. Both hybrid HF/DFT methods predict the N−N and C−N distances to within 0.01 Å from the experimental value. Furthermore, the angles around the nitrogen are calculated to be exactly equal to the experimental values, another example of the good performance of the B3PW91 and B3LYP methods.

The UV absorption spectrum of **2**++ in CH_3CN has maxima at 317 nm (ϵ 2600 M^{-1} cm^{-1}) and 227 nm (ϵ 8400 M^{-1} cm^{-1}).[26] The B3LYP/6-31G* TDDFT calculation yields a lowest excitation energy of 3.56 eV, corresponding to an absorption wavelength of 348 nm, with an oscillator strength of 0.035. The agreement with experiment is not as good as in the cases of **1**+ and **2**+ but is still satisfactory.

(B) Self-Exchange Electron-Transfer and Internal Reorganization Energies. Because of the stability of both the cation and dication of **2**, Nelsen and coworkers[43] were able to determine the rate constants k_{et} for the self-exchange electron transfer between **2** and **2**+ and **2**+ and **2**++ by ^{1}H NMR line broadening measurements in acetonitrile. Surprisingly, the rates for electron transfer in acetonitrile were extremely low, i.e. 7.0×10^2 M^{-1} s^{-1} for **2**/**2**+ and 2.1×10^4 M^{-1} s^{-1} for **2**+/**2**++. For the former system this is a factor 10^6 slower than the self-exchange electron transfer in 1,4-bis(dimethylamino)-benzene (commonly known as *N*,*N*,*N*′,*N*′-tetramethyl-*p*-phenylenediamine, TMPD) and its radical cation, a pair of molecules of similar size. For the **2**+/**2**++ pair, activation parameters could also be obtained. Internal reorganization energies were estimated earlier[43] using AM1 calculations on neutral, cation, and dication in a D_{2h} minimized structure. We can now compare these values with internal reorganization energies determined via DFT calculations.

The internal reorganization energy (λ_i) in the self-exchange process between, e.g., **2** and **2**+ is composed of two contributions, as illustrated in Figure 5. It is the sum of the energy gained when the radical cation changes its geometry from that of the neutral molecule to the

(43) Nelsen, S. F.; Blackstock, S. C.; Kim, Y. *J. Am. Chem. Soc.* **1987**, *109*, 677.
(44) Nelsen, S. F.; Frigo, T. B.; Kim, Y. *J. Am. Chem. Soc.* **1989**, *111*, 5387.

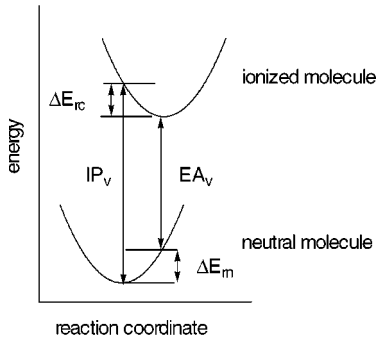

Figure 5. Schematic representation of potential energy curves versus reaction coordinate for self-exchange electron transfer. IP_v = vertical ionization energy of the neutral. EA_v = vertical electron affinity of the radical cation. ΔE_{rc} = difference between adiabatic and vertical ionization potential of the neutral. ΔE_{rn} = difference between the vertical and adiabatic electron affinity of the radical cation.

Table 3. Calculated Energies (eV) Relative to the Neutral Ground State of 2, 2+, and 2++

method	geometry	**2**	**2+**	**2++**
(U)B3LYP/6-31G*	neutral	0.00	5.94[a]	
	cation	0.79	5.13	16.28
	dication		5.34	15.92
AM1[b]	neutral	0.00	7.24[a]	
	cation	0.76	6.58	

[a] The experimental value is 6.36 eV.[44] [b] Values obtained from ref 43.

equilibrium geometry of the radical cation (i.e., the difference between the vertical and adiabatic ionization energy of the neutral (ΔE_{rc})) and the relaxation energy of the neutral molecule starting from the radical cation geometry (i.e., the difference of the vertical and adiabatic electron affinity of the cation (ΔE_{rn})).[43] Neglecting possible entropy effects, these energy differences can all be calculated with the geometrical results described in the preceding section and are listed in Table 3. The vertical ionization energy was determined by Nelsen and coworkers[44] to be 6.36 eV, which is considerably better calculated with DFT (B3LYP/6-31G*) than with AM1, as may be expected. Furthermore, in the AM1 calculations, the geometries were all assumed to have D_{2h} symmetry, which induces errors in the determination of the vertical ionization energy. Unfortunately, the adiabatic ionization potential is not available for the **2/2+** pair.

Using the Marcus expression for the activation energy (eq 1) of self-exchange electron transfer between a neutral molecule and its singly charged ion, the reorganization energy can be easily determined. On a purely experimental basis, the separate contributions of the internal reorganization energy λ_i and the solvent reorganization energy λ_s cannot be established. Usually, λ_s is estimated using continuum models, but this estimation requires several assumptions.

$$\Delta G^* = \frac{(\lambda_s + \lambda_i)}{4} \qquad (1)$$

The relevant electron transfer parameters are given in Table 4. The present ab initio calculations only give energy values at 0 K, while the experimentally relevant quantities are (Gibbs) free energies. The present approach does not allow the extraction of the thermal contributions to λ_i. The (more relevant) intramolecular

Table 4. Calculated and Observed Electron Transfer Parameters[a]

		computed			experimental		
	method	ΔE_{rc}	ΔE_{rn}	$\lambda_{i/4}$	k_{et} (M^{-1} s^{-1})	$\Delta G^{\ddagger}_{et}$	$\Delta H^{\ddagger}_{et}$
2/2+	B3LYP	18.6	18.2	9.2	7.0×10^2	13.4	
	AM1[b]	15.2	17.6	8.2	7.0×10^2	13.4	
2+/2++	B3LYP	8.3	4.8	3.3	2.1×10^4	11.5	8.5
	AM1[b]	9.7	5.1	3.7	2.1×10^4	11.5	8.5

[a] See text for meaning of symbols. All energies are given in kcal/mol. For the case of **2+/2++** ΔE_{rc} actually refers to the dication instead of the cation and ΔE_{rn} is the relaxation energy of the radical cation. [b] Values obtained from ref 43. The **2/2+** pair was measured at 23.0 °C in acetonitrile solution, whereas the **2+/2++** pair was measured at 24.1 °C.

vibrational contributions to the activation energy could in principle be estimated by calculations of the transition structure,[45−47] but this is beyond the scope of the present study. The experimental data for the **2+/2++** pair show that the activation entropy of the self-exchange electron transfer ($\Delta S^{\ddagger}_{et}$) is −10.3 cal mol^{-1} K^{-1}, which makes a quite significant contribution to the barrier.[43]

For the **2/2+** pair, the values for ΔE_{rc} are larger than the corresponding ΔE_{rn} values, i.e., the radical cation is more easily distorted than the neutral molecule. Plots of the asymmetry in these systems were calculated using AM1 by Nelsen et al.[43] for the **2/2+** and **2+/2++** pairs. The asymmetry for the **2/2+** pair is, however, different for the B3LYP calculation. ΔE_{rc} is calculated to be slightly larger than ΔE_{rn}, opposite with respect to the AM1 calculations. This does not affect the total internal reorganization energy: the value of $\lambda_i/4$ which is the contribution of the internal reorganization energy to the barrier of self-exchange electron transfer, obtained with our calculations, is about 1 kcal/mol higher than that calculated with AM1. Although the difference is only small, we tend to put more faith in the B3LYP value of 9.2 kcal/mol, because the structures calculated with B3LYP correspond much better with the X-ray structures than do the AM1 structures, and in general the B3LYP calculations also reproduce vibrational frequencies very well, in contrast to AM1. The value of 9.2 kcal/mol for $\lambda_i/4$ is already 69% of the value of $\Delta G^{\ddagger}_{et}$, which means that the internal reorganization energy λ_i is much larger than the solvent contribution λ_s in this system, a rather uncommon situation for electron transfer in polar solvents.

For the **2+/2++** pair, the internal reorganization energies are smaller than those for the **2/2+** pair due to the smaller geometry changes going from **2+** to **2++**. ΔE_{rc} and ΔE_{rn} differ considerably now, with ΔE_{rc} being about twice as large as ΔE_{rn}, from both B3LYP and AM1 calculations. This is due to the stiffness of the dication, which has a full π-bond between the nitrogen atoms.

The differences between the barrier heights and the contributions of internal reorganization energy ($\lambda_i/4$) are due to the solvent reorganization energy and, in the case of **2+/2++**, the electrostatic repulsion of the interacting ions (work term). Because the *change* in charge distribution in both one-electron transfer processes should be essentially the same, λ_s should be similar for both cases. The difference $\Delta G^{\ddagger}_{et} - \lambda_i/4$ (B3LYP) for **2+/2++** is 4 kcal/

(45) Farazdel, A.; Dupuis, M.; Clementi, E.; Aviram, A. *J. Am. Chem. Soc.* **1990**, *112*, 4206.
(46) Farazdel, A.; Dupuis, M. *J. Comput. Chem.* **1991**, *12*, 276.
(47) Rauhut, G.; Clark, T. *J. Am. Chem. Soc.* **1993**, *115*, 9127.

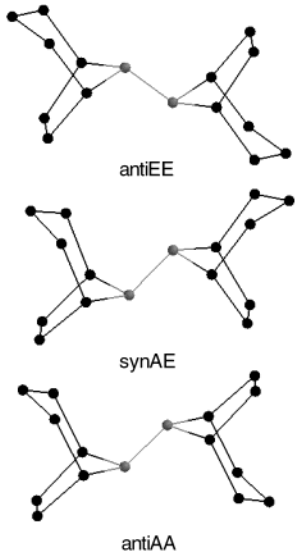

Figure 6. Conformational isomers of compound **3**. Hydrogen atoms not shown.

mol greater than that for the **2/2**+ pair. This appears a reasonable value for the work term, corresponding to the repulsion energy of point charges in acetonitrile at a distance of ca. 4.5 Å, consistent with the idea that the reactants have to be in close contact for electron transfer to occur. The solvent reorganization then contributes at most 4.2 kcal/mol to the barriers, probably less because a negative entropy of activation is inherently associated with bimolecular reactions and because the free energy barrier ΔG^* in Marcus theory is typically somewhat lower than the $\Delta G^{\ddagger}$ obtained experimentally by applying the Eyring rate expression.[48]

8,8′-Bis-8-azabicyclo[3.2.1]octane (3). Another hydrazine radical cation which could be crystallized as its nitrate salt is **3**+.[28] This hydrazine differs from **2** in the additional degree of freedom about the N−N bond. Crystal structures for the more highly symmetric 9,9′-bis-9-azabicyclo[3.3.1]nonane **4**[49] and tetraisopropylhydrazine **5**[23] have also been published, but these will not be discussed here. Because of the asymmetry in the substituents in principle three kinds of conformations can exist both in the neutral and the radical cation of **3**. The $(CH_2)_3$ bridges can be syn or anti with respect to each other, and the NN bond can be axial or equatorial with respect to the six-membered piperidine ring. This leads to the conformations for the neutral shown in Figure 6. Compound **3** crystallizes in its least favorable conformer in solution, the antiAA form, probably because this is the most compact form.[28] It has been shown by ^{13}C NMR in $CHCl_3$ at −70 °C that all conformations coexist in solution but that the antiEE conformation is 0.26 and 0.48 kcal/mol more stable than the syn and the anti-AA conformations, respectively.[28] B3LYP/6-31G* optimizations predict the antiEE conformation to have the lowest energy; the antiAA and syn conformations are higher in calculated energy by 0.56 and 0.70 kcal/mol, respectively. When thermal corrections based on the harmonic vibrational frequencies are taken into account, the relative free energies at 223 K of the syn and antiAA forms are +0.26 and +1.30 kcal/mol, respectively.

Table 5. Experimental and B3PW91/6-31G* Calculated Features of 8,8′-Bis-8-azabicyclo[3.2.1]octane Neutral and Radical Cation (antiAA Conformation)[a]

	neutral **3**		radical cation **3**+	
	exp	B3PW91	exp	B3PW91
r(N−N)	1.469	1.452	1.323	1.333
r(C−N)	1.484	1.481	1.486	1.482
∠(C_1−N−N)	111.2	112.0	120.7	121.4
∠(C_1−N−$C_{1'}$)	101.3	101.6	105.5	105.2
ΣN	323.7	325.6	346.9	348.0
∠(N−C_1−C_2)	100.2	100.2	100.5	100.7
∠(N−C_1−C_3)	112.9	112.6	106.9	107.6
ENDOR data				
a_N(2)			13.7	13.2
a_H(4)(C1)			4.5	4.5
a_H(2)(C_4,eq)			3.43	3.6
a_H(4)(C_3,eq)			1.03	1.3

[a] Crystallographic and ENDOR data from Nelsen et al. for **3** and **3**+(•NO_3^-).[28] For atom numbering see Figure 1. Bond distances in Å, angles in degrees. Hyperfine interaction constants in Gauss. Results computed with other methods can be found in the Supporting Information.

The geometrical features calculated at the B3PW91/6-31G* level for the antiAA conformer are compared with the crystal structure in Table 5. Data obtained with other methods can be found in the Supporting Information (Table S5). The B3LYP and B3PW91 methods show the best overall results. The pure DFT methods predict the pyramidalization around the nitrogens, measured as the sum of the bond angles, best. The bond distances, however, are too large. The pyramidalization of the nitrogens is calculated to be 4° too large in the HF calculation.

Upon oxidation of **3** various characteristic geometry changes are observed. The nitrogens are flattened with respect to the neutral, which is due to the presence of net π-bonding interaction after ejecting one electron from the π-antibonding HOMO, similar to the case of **2**+. The increase of the N−N bonding interaction leads to a drastic decrease of the N−N bond length from 1.47 Å in the neutral to 1.32 Å in the radical cation. The sum of the nitrogen bond angles ΣN increases as well from 323.7° in the neutral molecule to 346.9° in the radical cation. Like the neutral molecule, the radical cation crystallized in the anti-AA form. Also in solution this is the most stable conformation as was deduced from ENDOR hydrogen splittings.[28] The syn conformation is calculated (UB3LYP/6-31G*) to be 2.4 kcal/mol higher in energy than the anti form, a somewhat larger difference than the experimental value of 1.5 kcal/mol. The UV absorption maximum of the anti conformer is at 337 nm; that of the syn conformer is at 318 nm.[50] The TDDFT/B3LYP/6-31G* excitation energies are in reasonably good agreement (anti: 3.87 eV (321 nm), $f = 0.14$; syn: 4.11 eV (302 nm), $f = 0.15$) and certainly reflect the difference between the conformational isomers very well. This difference in excitation energies is due to the properties of the doubly occupied N−N bonding MO. In the anti form this is of relatively high energy because the lone pairs are in a more or less equatorial orientation and are forced into an unfavorable interaction with the C−C σ bonding MOs of the six-membered ring. In the syn form, in which one of the lone pairs is axially oriented, this unfavorable interaction is smaller. The extent of nitrogen pyramidal-

(48) Nelsen, S. F. *Adv. Electron Transfer Chem.* **1993**, *3*, 168.
(49) Nelsen, S. F.; Hollinsed, W. C.; Kessel, C. R.; Calabrese, J. C. *J. Am. Chem. Soc.* **1978**, *100*, 7876.
(50) Nelsen, S. F.; Blackstock, S. C.; Yumibe, N. P.; Frigo, T. B.; Carpenter, J. E.; Weinhold, F. *J. Am. Chem. Soc.* **1985**, *107*, 143.

ization in the two forms, which Nelsen et al.[50] held responsible for the difference in excitation energies, is very small.

The nitrogen splitting constant of 13.7 G obtained from the ENDOR study is calculated accurately by all DFT methods, particularly by B3LYP, which also reproduces the hydrogen splittings very well. This illustrates together with the other calculated geometrical features the excellent performance of the two hybrid HF/DFT methods. Nelsen et al. argue on the basis of the observed and calculated splittings of the bridgehead hydrogens (C_1) that the nitrogens of **3**+ should be less pyramidal in solution than in the crystal. The good agreement of the present calculated results, which represent the isolated molecule, with structural features in the crystal and spectroscopic features determined in solution, however, do not support this view.

Concluding Remarks

In this investigation it was shown that the molecular structures as well as electronic properties of three different open-shell diaza systems can be quite accurately calculated using modern ab initio density functional calculations. Even subtle structural and spectroscopic differences, e.g., in the excitation energies of the conformers of **3**+, are accounted for very well. Our results support the idea that this kind of calculation can give reliable evidence for the structure of the molecule in the absence of experimental data on the crystal or gas-phase structure. Despite the encouraging results, it should be kept in mind that DFT still fails in some cases. For example, DFT methods are known to overestimate electron delocalization; but this is not a problem in the present case.

It was demonstrated that in most cases the Hartree−Fock method underestimates the N−N bond distance considerably in the radical cations and even more in the dications. Although HF is still an attractive method because it is computationally efficient, its results are unsatisfactory in some cases. The performance of the pure density functional methods, BLYP and BPW91, is similar. Both underestimate the N−N bonding interactions, although the BPW91 method generally performs better than BLYP. Of all the methods tested, the B3PW91 method gives the best results. It performs slightly better than the more commonly used B3LYP method and is therefore recommended for use for systems like those studied in the present work. In the recent literature, several new density functionals have been reported which offer both a more satisfactory theoretical foundation and a performance that can be systematically somewhat better than that of B3LYP or B3PW91.[51−57]

The (U)B3LYP calculations of the internal reorganization energies of self-exchange electron transfer for the **2**/**2**+ and **2**+/**2**++ pairs highlight another interesting result of the present study. As in our previous work,[14,18] the calculated internal reorganization energies agree well with experimental data. In many other electron transfer studies these molecular parameters are not so easily available experimentally, so the possibility of calculating them using standard and widely available ab initio methods should be very useful.

The results of time-dependent DFT calculations of excitation energies and oscillator strengths are encouraging. The agreement with experimental results in most cases is very good.

In subsequent papers we will subject the DFT calculations to a severe test by investigating their performance in asymmetric piperazine radical cations,[21] in which agreement between computed and experimental results will depend strongly on the ability of DFT to correctly estimate the degree of delocalization of spin and charge.

Acknowledgment. The authors thank Prof. Jan W. Verhoeven for valuable discussions.

Supporting Information Available: Tables S1−S5 containing additional computed data of compounds **1**, **2**, and **3** and their radical cations and dications. Calculated energies and Cartesian coordinates of all computed structures. This material is available free of charge via the Internet at http://pubs.acs.org.

JO005605S

(51) Schmider, H. L.; Becke, A. D. *J. Chem. Phys.* **1998**, *109*, 8188.
(52) Adamo, C.; Barone, V. *J. Chem. Phys.* **1998**, *108*, 664.
(53) Hamprecht, F. A.; Cohen, A. J.; Tozer, D. J.; Handy, N. C. *J. Chem. Phys.* **1998**, *109*, 6264.
(54) Tozer, D. J.; Handy, N. C. *J. Chem. Phys.* **1998**, *108*, 2545.
(55) Bienati, M.; Adamo, C.; Barone, V. *Chem. Phys. Lett.* **1999**, *311*, 69.
(56) Adamo, C.; Barone, V. *J. Chem. Phys.* **1999**, *110*, 6158.
(57) Becke, A. D. *J. Chem. Phys.* **2000**, *112*, 4020.